Methods 114 (2017) 28–38

Contents lists available at ScienceDirect

Methods

journal homepage: www.elsevier.com/locate/ymeth

Quantitative telomeric chromatin isolation protocol for human cells

Jana Majerská, Sophie Redon, Joachim Lingner *

Swiss Institute for Experimental Cancer Research (ISREC), School of Life Sciences, Ecole Polytechnique Fédérale de Lausanne (EPFL), 1015 Lausanne, Switzerland

ARTICLE INFO

Article history:
Received 27 May 2016
Received in revised form 19 July 2016
Accepted 7 August 2016
Available online 9 August 2016

Keywords:
Telomeres
Chromatin
Mass spectrometry
Affinity purification
SILAC

ABSTRACT

The ends of eukaryotic chromosomes, known as telomeres, consist of repetitive DNA sequences, multiple proteins and noncoding RNAs. Telomeres are dynamic structures that play crucial roles as guardians of genome stability and tumor suppressors. Defects in telomere length or protein composition can accelerate aging and are seen in telomere syndromes, which affect various proliferative tissues such as the bone marrow or the lungs. One of the biggest challenges in the telomere field is to identify the molecular changes at telomeres that occur during normal development, in cancer and in telomere syndromes. To tackle this problem, our laboratory has established a quantitative telomeric chromatin isolation protocol (QTIP) for human cells, in which chromatin is cross-linked, immunopurified and analyzed by mass spectrometry. QTIP involves stable isotope labeling by amino acids in cell culture (SILAC) to compare and identify quantitative differences in telomere protein composition of cells from various states.

1. Introduction

The functions of telomeres rely on their constituents, which include telomeric DNA, telomeric proteins and the telomeric long noncoding RNA TERRA. Telomeric DNA consists of simple repetitive DNA sequences (5′-TTAGGG-3′/5′-CCCTAA-3′ repeats in vertebrates) of several kilobases and terminates with single-stranded 3′ overhangs measuring a few hundred nucleotides. Telomeric DNA is assembled with specialized telomere binding proteins. They include six abundant telomere-specific proteins referred to as shelterins [1]. The shelterin components TRF1 and TRF2 both bind directly to the double stranded portion of telomeric DNA as homodimers. POT1 binds to the telomeric 3′ overhang [2]. TIN2, TPP1 and Rap1 associate with telomeres through protein interactions with TRF1, TRF2 and POT1. Shelterin components are crucial for protection of chromosome ends from fusion and recombination events and for suppressing a DNA damage response at telomeres, which triggers cell cycle arrest and cellular senescence [1,3]. TRF2 dysfunction leads to high rates of chromosome end-to-end fusions, which are detrimental to chromosome segregation during mitosis. TRF1 is critical for efficient semiconservative telomeric DNA replication as in its absence replication forks frequently stall or collapse [4,5]. The shelterin components also regulate telomere length and telomerase recruitment. For example, TPP1 binds telomerase and recruits telomerase to telomeres in S phase of the cell cycle to promote telomere elongation [6–9]. Notably, mutations in TIN2, TPP1 and POT1 have been linked to telomeropathies in which telomere length and structure may be perturbed [10–14]. POT1 mutations were also observed in various cancers (e.g. Ref. [15]) inducing telomere replication stress [16]. Other important telomere factors are involved in the regulation of telomerase. For example, the recently discovered mammalian CST complex is thought to play critical roles in semiconservative DNA replication of telomeric DNA in conjunction with shelterin proteins, in addition to restricting telomerase to single binding and extension events [17–22]. Mutant forms of the CTC1 subunit of the CST complex have been linked to the telomeropathies Coats Plus and Dyskeratosis congenita [23–26].

Telomeres are transcribed into the long noncoding RNA TERRA [27–29]. TERRA transcription starts from promoters in the subtelomeric region and proceeds towards chromosome ends. TERRA sustains several important functions at chromosome ends (reviewed in [28]). TERRA promotes protein composition changes at telomeres. For example, it assists recruitment of the chromatin modifiers LSD1 (a lysine demethylase) and SUV39H1 (a histone H3 lysine 9 methylase) to damaged telomeres thereby enabling DNA end processing [30,31] and it has also been proposed to promote telomere protein composition changes during cell cycle progression [32]. TERRA can regulate telomere length through modulation of exonuclease 1 and telomerase [33,34]. Abnormally high levels of TERRA at telomeres interfere with telomere maintenance in human cells as seen in RNA surveillance mutants [27]. In ICF (immunodeficiency, centromeric instability, facial anomalies) patient-derived cell lines which lack DNA methyl transferase 3b [35], subtelomeric CpG islands are undermethylated which

* Corresponding author.
E-mail address: joachim.lingner@epfl.ch (J. Lingner).

http://dx.doi.org/10.1016/j.ymeth.2016.08.003
1046-2023/

presumably leads to TERRA overexpression in these patients. ICF patients have extremely short telomeres.

In addition to shelterin, CST and TERRA binding proteins, an increasingly large number of low abundant proteins has been found in association with telomeres. These proteins also perform crucial functions as they are mutated in several fatal degenerative syndromes. Several DNA helicases including the Werner protein (mutated in Werner syndrome), RTEL1 (mutated in telomeropathies), Pif1, and BLM (mutated in Bloom's syndrome) are critical for the faithful semiconservative DNA replication of telomeric DNA. They may unwind G-quadruplex DNA structures, in which four guanine bases of the telomeric G-strand associate through Hoogsteen hydrogen bonding to form tetrads [36–39]. In addition, RTEL1 unfolds t-loop structures [40]. In the t-loop structure, telomeres are found in a lariat conformation, which involves strand invasion of the 3′ single-stranded telomeric overhang into the double-stranded telomeric DNA [41]. Using the quantitative telomeric chromatin isolation protocol (QTIP) described below, we identified the THO complex associated with telomeres where it suppresses the formation of TERRA RNA/telomeric DNA hybrid structures (so-called R-loops) [42,43].

Telomeric protein composition has not been determined in a comprehensive and accurate manner. Indeed, approximately one third of the patients suffering from telomeropathies carry mutations in unknown genes suggesting that a considerable number of functionally important telomeric proteins remain to be discovered and characterized. In addition, little is known on how the telomere composition changes in disease. Thus, QTIP should allow addressing fundamental questions regarding telomere composition and function in the future.

2. Materials and methods

2.1. Preparation of anti-TRF1 and anti-TRF2 specific antibodies for QTIP

2.1.1. Expression and purification of recombinant TRF1 and TRF2

Recombinant TRF1 and TRF2 proteins with N-terminal His_6- and S-tags were expressed in Rosetta(DE3)pLysS *E. coli* (Novagen, 70956-4) from pET-30a(+)-derived plasmids (gifts from Daniela Rhodes [42]). Cultures were grown to an OD_{600} of 0.8–0.9 at 25 °C in 2xYT medium supplemented with 25 μg/ml kanamycin (Applichem). Expression of the recombinant proteins was induced by the addition of 0.4 mM isopropyl-β-D-thiogalactopyranoside (IPTG; Applichem) at 15 °C overnight. The bacteria were harvested by centrifugation and the pellets resuspended in resuspension buffer (50 mM HEPES-NaOH pH 8.0, 500 mM KCl, 1% Triton X-100, 10 mM β-mercaptoethanol, 1 mM phenylmethylsulfonyl fluoride (PMSF)). The cells were lysed by sonication (Branson Sonifier 250, output 2.8, 3–5 cycles, 30 s of operation and 30 s of rest per cycle) on ice and sonicated bacterial extracts were cleared by centrifugation (10,000 g for 30 min at 4 °C). The recombinant proteins were purified from the extracts by Ni^{2+} affinity chromatography (Ni-NTA agarose, Qiagen) according to manufacturer's instructions. After 5 washes with 50 mM HEPES-NaOH pH 8.0, 500 mM KCl, 20 mM imidazole, 10% glycerol, 10 mM β-mercaptoethanol, 1 mM PMSF, the purified proteins were eluted with high-salt high-imidazole buffer (50 mM HEPES-NaOH pH 8.0, 2 M KCl, 500 mM imidazole, 1% NP-40, 20 mM EDTA-NaOH pH 8.0, 10% glycerol, 10 mM β-mercaptoethanol, 1 tablet/50 ml EDTA-free protease inhibitor cocktail (Roche #05056489001)). The proteins were dialyzed against 1× phosphate-buffered saline (PBS), 10% glycerol (SnakeSkin Pleated Dialysis Tubing, 10 kDa cutoff, Thermo Fisher Scientific Group) and concentrated on Amicon Ultra centrifugal filters (30 kDa, Merck Millipore UFC903024). The integrity and purity of recombinant proteins were assessed on SDS–PAGE gels that were stained with Coomassie Brilliant Blue and probed for TRF1 and TRF2 by Western blotting.

2.1.2. Generation of anti-TRF1 and anti-TRF2 specific antibodies

For anti-TRF1 and anti-TRF2 antibodies, rabbits were immunized with purified full-length His_6-S-TRF1 and His_6-S-TRF2, respectively (Eurogentec). The rabbits received four injections (on days 0, 14, 28 and 56) of 120 μg of purified protein during a 87-day program. The serum obtained from the final bleeds (day 87) was used for antibody purification.

Anti-TRF1 and anti-TRF2 antibodies were affinity-purified from rabbit sera using the respective antigens coupled to an Affigel matrix (Bio-Rad): His_6-S-TRF1 (pI = 6.0) was coupled to Affigel 15 (suitable for proteins with pI below 6.5), while His_6-S-TRF2 (pI = 9.22) was coupled to Affigel 10 (for proteins with pI 6.5–11). 1 ml Affigel was washed with H_2O and added to 14 ml Biorad columns. 5 mg of purified protein in 10 ml 1× PBS was coupled to Affigel for 4 h at 4 °C on a wheel. Unbound protein was drained by gravity. The beads were blocked with 3 ml of 0.1 M ethanolamine for 1 h at 4 °C and quickly washed with 3 ml of 0.2 M glycine-HCl pH 2.5, 0.5 M NaCl. The beads were washed with 20 ml cold 1× PBS and after addition of 0.02% sodium azide stored at 4 °C for up to one year.

The antigen-coupled beads were incubated with 5 ml of serum at 4 °C for 4 h to overnight. The beads were washed twice with 10 ml of 1× PBS and antibodies were eluted in 8–10 rounds with 1 ml 0.1 M glycine-HCl pH 2.5, 0.5 M NaCl. The eluted antibodies were immediately neutralized with 1 M sodium phosphate buffer pH 8.0. After elution, beads were rinsed twice with 10 ml 1× PBS and stored at 4 °C for reuse. The OD at 280 nm was determined for each fraction. Antibody containing fractions were pooled and dialyzed against 1× PBS, 10% glycerol. The affinity purified antibodies were stored in 1× PBS, 50% glycerol at −20 °C (or in 1× PBS, 10% glycerol at 4 °C).

2.1.3. Activity and specificity analysis of anti-TRF1 and anti-TRF2 antibodies by ChIP

In order to optimize antibody concentration for QTIP, antibodies were titrated in small-scale ChIP experiments using the corresponding cell lines. In the provided example, experimentally transformed [44] human lung fibroblasts [45] were crosslinked in suspension using 1% formaldehyde in PBS for 10 min at 25 °C. The crosslinking reaction was quenched 5 min at 25 °C by adding glycine to a final concentration of 125 mM. The cells were washed three times in PBS, resuspended in lysis buffer (50 mM Tris-HCl pH 8.0, 1% SDS, 10 mM EDTA-NaOH pH 8.0, EDTA-free protease inhibitor complex (Roche); 1 ml per 10^6 cells) and incubated for 5 min at 25 °C. The lysate was centrifuged for 5 min at 1,500 g and the pellet washed in LB3 buffer (10 mM Tris-HCl pH 8.0, 200 mM NaCl, 1 mM EDTA-NaOH pH 8.0, 0.5 mM EGTA-NaOH pH 8.0, 0.1% sodium-deoxycholate, 0.25% sodium lauroyl sarcosinate, EDTA-free protease inhibitor complex (Roche); 1 ml per 10^6 cells) and centrifuged as above. The chromatin-enriched pellet was resuspended in LB3 buffer (1 ml per 2×10^7 cells) and sonicated for 12 min at 4 °C using a Focused-Ultrasonicator (E220, Covaris, duty: 5.0, PIP: 140, cycles: 200, amplitude: 0, velocity: 0, dwell: 0, 12 × 12-mm glass tubes with AFA fiber). The sonicated extracts were centrifuged at 4 °C for 15 min at 20,000 g to remove insoluble material. The supernatant was mixed 1:1 with ChIP dilution buffer (50 mM Tris-HCl pH 8.0, 600 mM NaCl, 0.75% Triton X-100, 10 mM EDTA-NaOH pH 8.0, EDTA-free protease inhibitor complex (Roche)) and pre-cleared for 1 h at 4 °C with Sepharose 6B (Sigma) that had been pre-blocked for 1 h at 4 °C with 1 mg of yeast tRNA per 1 ml of 50% bead slurry. For each IP reaction, the pre-cleared lysate corresponding to 2×10^6 cells was supplemented with 0–4 μg of affinity

purified anti-TRF1, anti-TRF2, 1:1 mixtures of anti-TRF1 and anti-TRF2, or normal rabbit IgG (sc-2027, Santa Cruz Biotechnology), and incubated overnight at 4 °C on a rotating wheel. 40 µl of 50% slurry of Protein G Sepharose 4 Fast Flow (pre-blocked with yeast tRNA as above) was added and the samples were further incubated at 4 °C for 1 h. Beads were washed as in QTIP. The DNA was eluted by incubating the beads overnight at 65 °C in 100 µl of crosslink reversal buffer (20 mM Tris-HCl pH 8.0, 0.1 M $NaHCO_3$, 1% SDS, 0.5 mM EDTA-NaOH pH 8.0, 10 µg DNase-free RNase (Roche)). The DNA was purified with the QIAquick PCR Purification kit (Qiagen) and analyzed by dot-blot hybridization as described in Section 2.4.

2.1.4. Coupling of antibodies to protein G Sepharose beads

For QTIP, the antibodies were covalently linked to Protein G Sepharose in order to prevent their leakage into the telomeric chromatin fractions. 3–4 µl of 50% bead slurry per 10^6 cells was used. Protein G Sepharose 4 Fast Flow beads (GE Healthcare Bio-Sciences 17-0618-05) were washed four times with ten volumes of cold 1× PBS and combined with antibodies (typically, 0.2–0.45 µg anti-TRF1+0.2–0.45 µg anti-TRF2/µl bed volume). The reaction volume was adjusted to 10 bead bed volumes with 1× PBS and incubated for 3 h at 4 °C on a rotating wheel. The beads with bound antibodies were washed twice with 10 volumes of 0.2 M sodium borate pH 9.0 (sodium tetraborate decahydrate, Sigma) and resuspended in 10 volumes of 0.2 M sodium borate pH 9.0 containing freshly added 20 mM dimethyl pimelimidate dihydrochloride (DMP, Sigma D8388). Coupling reactions were performed for 30 min at 25–30 °C on a rotating wheel. To stop the reaction, the beads were washed with 10 volumes of 0.2 M ethanolamine pH 8.0, followed by a 2 h incubation in 10 volumes of 0.2 M ethanolamine pH 8.0 at room temperature. The beads were washed 3 times with cold 1× PBS, resuspended in 20 mM Tris-HCl pH 8.0, 150 mM NaCl and upon addition of 0.02% sodium azide, stored at 4 °C for up to one year. Coupling efficiency was tested by SDS-PAGE analysis of representative samples taken before and after coupling. The activity of antibody-coupled beads was verified in small-scale ChIP experiments.

2.2. Cell culture conditions and stable isotope labeling with amino acids

2.2.1. Reagents for SILAC labeling

- Cell line of choice: In the provided example, we used HeLa and HeLa super-telomerase cells that carried over-elongated telomeres [42,46].
- SILAC-compatible growth medium without L-lysine and L-arginine: e.g. DMEM medium for SILAC (Thermo Scientific #89985). VP-6 (InVitrus™) or RPMI-1640 can be used for cell lines grown in suspension.
- Dialyzed fetal bovine serum (FBS, Thermo Scientific #88440).
- Amino acids: light lysine: L-lysine-2HCl ($^{12}C/^{14}N$,Thermo Scientific #88429), light arginine: L-arginine-HCl ($^{12}C/^{14}N$, Thermo Scientific #88427), light proline: L-proline (Thermo Scientific #88430), heavy lysine K8: L-lysine-2HCl ($^{13}C/^{15}N$; Cambridge Isotope Laboratories CNLM-291-H), heavy arginine R10: L-arginine-HCl ($^{13}C/^{15}N$; Cambridge Isotope Laboratories CNLM-539-H).
- Penicillin-Streptomycin (10,000 U/ml; Gibco #15140-122).
- Trypsin-EDTA (0.05%, Gibco #25300-054).

2.2.2. General considerations

All amino acids were prepared as concentrated stock solutions (e.g. 100 mg/ml) in 1× PBS and the aliquots were stored at −20 °C. Before use, the growth medium was supplemented with dialyzed FBS, antibiotics and amino acids at the desired concentration, and filtered through a 0.22 µm filter. The complete medium was stored at 4 °C for up to one month. FBS was dialyzed to eliminate unlabeled amino acids [47]. Since some cell lines are sensitive to the loss of dialyzable small molecules, careful monitoring of growth characteristics and cell behavior is necessary. If required, the SILAC medium can be supplemented with purified growth factors or a small percentage of normal serum. To ensure complete labeling of even long-lived proteins, cells should be grown in SILAC medium for at least five population doublings. The efficiency of metabolic labeling may be determined by mass spectrometry analysis of aliquots of heavy-labeled whole cell lysates from 4 to 12 population doublings. The isotopic enrichment of heavy arginine and heavy lysine should exceed 98%. Some cell types have the ability to convert arginine to proline (and *vice versa*), resulting in accumulation of isotopically labeled proline residues and erroneous quantitation of proline-containing peptides. The arginine-to-proline conversion can be minimized (<2%) by adding light proline to the heavy SILAC medium. Therefore, titration experiments of arginine and proline must be performed [48]. An alternative solution is to use lysine-only labeling in combination with Lys-C digestion instead of trypsin. The medium should be changed every 2–3 days if the cells are not ready for subculture. When cells are detached with trypsin for subculturing, they should be centrifuged and washed with PBS since residual trypsin is the source of unlabeled amino acids reducing incorporation efficiency of heavy amino acids. The two cell populations to be compared should be grown in parallel under identical conditions. Label-swap experiments in which the heavy and light media are exchanged between the two cell populations allow straightforward identification of contaminating proteins that come from the environment as they contain only light amino acids.

2.2.3. Conditions for HeLa cells

Unlabeled HeLa cells were maintained in DMEM (Gibco) containing 10% FBS (Gibco), 100 U/ml penicillin and 100 µg/ml streptomycin at 37 °C in a humidified incubator containing 5% CO_2. For SILAC labeling, HeLa cells were cultured in SILAC DMEM containing 10% dialyzed FBS, 100 U/ml penicillin, 100 µg/ml streptomycin, 200 mg/l proline, 25 mg/l $^{12}C/^{14}N$ arginine and 46 mg/l $^{12}C/^{14}N$ lysine (or an equimolar concentration of $^{13}C/^{15}N$ arginine and $^{13}C/^{15}N$ lysine). After five population doublings, cellular proteins had been labeled to near completion as assessed by mass spectrometry.

2.3. Quantitative telomeric chromatin isolation protocol (QTIP)

2.3.1. Reagents and equipment for QTIP

- Formaldehyde: 16% w/v solution methanol-free (Thermo Scientific #28908), single use ampules.
- Ethylene glycol bis(succinimidyl succinate) (EGS, Thermo Scientific #21565): 0.5 M solution in DMSO freshly prepared before use.
- 2 M Glycine in PBS; filtered.
- Lysis buffer: 50 mM Tris-HCl pH 8.0, 1% w/v SDS, 10 mM EDTA-NaOH pH 8.0; filtered. EDTA-free protease inhibitor complex (Roche) is added immediately prior to use.
- LB3 buffer: 10 mM Tris-HCl pH 8.0, 200 mM NaCl, 1 mM EDTA-NaOH pH 8.0, 0.5 mM EGTA-NaOH pH 8.0, 0.1% w/v sodium-deoxycholate (Fluka 30970), 0.25% w/v sodium lauroyl sarcosinate (Sigma L9150), EDTA-free protease inhibitor complex (Roche); prepared freshly before use, kept on ice.
- Sonicator: Focused-Ultrasonicator (E220, Covaris) + 12 × 12-mm glass tubes with AFA fiber (Covaris 520130); or Bioruptor (Diagenode).

- Sepharose 6B (Sigma) for pre-clearing.
- Affinity purified antibodies covalently coupled to protein G Sepharose beads (see Section 2.1).
- ChIP dilution buffer: 50 mM Tris-HCl pH 8.0, 0.75% Triton X-100, 10 mM EDTA-NaOH pH 8.0, 600 mM NaCl; filtered. EDTA-free protease inhibitor complex (Roche) is added prior to use.
- Yeast tRNA (Roche 10109509001).
- Wash buffer 1: 20 mM Tris-HCl pH 8.0, 0.1% w/v SDS, 1% Triton X-100, 2 mM EDTA-NaOH pH 8.0, 300 mM NaCl; filtered.
- Wash buffer 2: 20 mM Tris-HCl pH 8.0, 0.1% w/v SDS, 1% Triton X-100, 2 mM EDTA-NaOH pH 8.0, 500 mM NaCl; filtered.
- Wash buffer 3: 10 mM Tris-HCl pH 8.0, 250 mM LiCl, 1% w/v nonylphenylpolyethylene glycol (Nonidet P40 substitute; Applichem A1694), 1% w/v sodium-deoxycholate, 1 mM EDTA-NaOH pH 8.0; filtered.
- Wash buffer 4: 10 mM Tris-HCl pH 8.0, 1 mM EDTA-NaOH pH 8.0; filtered.
- Ammonium hydroxide (Sigma 221228): 0.25 M solution, freshly prepared.
- Mobicol Classic 1 ml columns (MoBiTec #M1003) with small 35 μm pore size filters (MoBiTec #M513515).
- Speedvac.
- Crosslink reversal buffer: 20 mM Tris-HCl pH 8.0, 1% w/v SDS, 0.1 M $NaHCO_3$, 0.5 mM EDTA-NaOH pH 8.0; filtered. 10 μg/ml DNase-free RNase (Roche #11119915001) is added prior to use.
- 4× SDS-PAGE loading buffer: 250 mM Tris-HCl pH 6.8, 40% glycerol, 8% w/v SDS, 10% β-mercaptoethanol, 0.04% w/v bromophenol blue; filtered.
- Mini-PROTEAN TGX Precast Gels 10%, 10-well comb, 50 μl/well (BioRad #456-1034).
- Gel electrophoretic apparatus: e.g. Bio-Rad Mini Protean 3 system.
- 10× SDS-PAGE running buffer: 250 mM Tris-HCl, 1.92 M glycine, 1% SDS.
- Simply Blue Safe Stain (Invitrogen LC6060).
- 0.22 μm filters: e.g. Stericup-GP sterile vacuum filtration system, 0.22 μm (Millipore, SCGPU05RE).

2.3.2. Cell harvest and chemical crosslinking

Adherent cell lines were typically grown in 150 cm^2 Petri dishes. Depending on the cell type, one confluent 150 cm^2 dish contains 5–40 × 10^6 cells. We used 50–500 × 10^6 cells per condition depending on telomere length and cell line. Subconfluent cells were detached by trypsinization and collected. Cells from the two conditions should be harvested in parallel, in the shortest possible time. Cell numbers were determined with an automated cell counting device (Casy, Schärfe Systems) or a hemocytometer (Neubauer chamber). Cells were diluted to identical concentrations. Light- and heavy-labeled cells were mixed in a 1:1 ratio (or according to telomeric chromatin content) and washed thoroughly in 1× PBS. The cells were resuspended in PBS (10^6 cells/ml) in Falcon tubes, and formaldehyde was added to a final concentration 1%. If dual crosslinking was desired, 2 mM EGS was added in addition to formaldehyde. After a short incubation (typically 10–20 min) at the optimized temperature (25 °C or 30 °C), the cross-linking reaction was quenched 5 min at 25 °C upon addition of glycine to a final concentration of 125 mM. The cells were collected by centrifugation (5 min at 400 *g* and 4 °C) and the pellets washed three times with cold 1× PBS. The crosslinked cell pellets were quick-frozen in liquid nitrogen and stored at −80 °C.

2.3.3. Lysis and chromatin enrichment

Frozen cell pellets were quick-thawed in a water bath at room temperature and resuspended in lysis buffer (10 × 10^6 cells per ml). Following a 5 min incubation on a wheel at 25 °C, the lysates were centrifuged at 1,500 *g* for 5 min, obtaining a transparent, gelatinous pellet containing insoluble chromatin.

2.3.4. Sonication

Sonication conditions should be optimized for each cell type and instrument. We provide two alternative protocols, for the use of a Bioruptor (Diagenode) or a Focused Ultrasonicator (E220, Covaris). The provided sonication conditions were optimized for HeLa cells crosslinked with 1% formaldehyde for 15 min at 30 °C.

For Bioruptor usage, the chromatin-enriched pellets from step 2.3.3 were washed once with lysis buffer, resuspended in lysis buffer (20 × 10^6 cells/ml), added to 50 ml Falcon tubes (7 ml/tube) and sonicated at 6 °C during 30–40 cycles with 30 s of operation and 30 s of rest per cycle. The presence of SDS greatly enhanced the sonication efficiency with Bioruptor but can lead to undesirable precipitation of material. Therefore, LB3 buffer which does not contain SDS can also be used.

For sonication with the Focused-Ultrasonicator, the chromatin-enriched pellets were washed once with cold LB3 buffer and resuspended in LB3 (25 × 10^6 cells/ml), aliquoted into 1 ml sonication vials (12 × 12-mm glass tubes with AFA fiber) and sonicated for 30 min at 4 °C (duty: 5.0, PIP: 140, cycles: 200, amplitude: 0, velocity: 0, dwell: 0). The sonication profiles obtained with the Focused-Ultrasonicator were not sensitive to cell concentration in a range of 8–30 × 10^6 cells/ml. The sonicated extracts were centrifuged at 20,000 *g* for 15 min at 4 °C and the supernatant transferred to a fresh tube. A very small opaque pellet, if any, is expected. Larger pellet sizes indicate poor sonication and insufficient solubilization of chromatin (over-crosslinking/under-sonication/too much starting material). It is crucial to analyze sonication efficiency by determining the DNA fragment sizes. For this, small aliquots of sonicated chromatin were put aside (0.1–0.3 × 10^6 cell equivalents), the crosslinks were reversed (overnight incubation in crosslink reversal buffer at 65 °C) and DNA was purified (QIAquick PCR Purification Kit, Qiagen) and analyzed on 1% agarose gels. DNA fragment sizes should range from 200 to 600 bp. Alternatively, DNA fragment lengths can be analyzed with a Bioanalyzer.

2.3.5. Chromatin immunoprecipitation

In order to obtain appropriate concentrations of detergents, Bioruptor-sonicated samples in lysis buffer were diluted 1:2 with ChIP dilution buffer, while Focused Ultrasonicator-sonicated samples in LB3 buffer were diluted 1:1 with ChIP dilution buffer. Sample concentrations ranged from 7 to 15 × 10^6 cell equivalents per ml of IP reaction. Samples were pre-cleared for 1–2 h at 4 °C with Sepharose 6 beads (1 ml 50% bead slurry per 200 × 10^6 cell equivalents) to remove background material that sticks nonspecifically to the beads. Pre-cleared samples were split and either added to beads coupled with nonspecific IgGs or beads coupled to affinity purified anti-TRF1 and/or anti-TRF2 antibodies. Prior to use, the beads were blocked for 1 h at 4 °C with 1 mg/ml yeast tRNA in ChIP dilution buffer. Typically, we used 3–4 μl of 50% bead slurry per 10^6 cells depending on titration experiments with antibody crosslinked beads. The immunoprecipitation was performed overnight at 4 °C. The beads were washed once with 10 bead volumes of wash buffer 1, once with wash buffer 2, once with wash buffer 3 and twice with wash buffer 4. For each wash, the samples were incubated for 5 min at 4 °C on a rotating wheel. The immunoprecipitated complexes were eluted in 2–3 rounds using 2.5 bead volumes of 0.25 M ammonium hydroxide incubated with the beads for 15 min at 37 °C with gentle agitation. At the end of the incubation, the samples were centrifuged and the supernatant was filtered through Mobicol columns to remove remaining beads. Eluates were combined and vacuum-dried. Samples were dissolved in 30 μl 1× PBS, 10 μl of 4× SDS-PAGE loading buffer was added, and the samples were heated to 95 °C for 30 min to reverse formaldehyde

crosslinks. For samples that had been crosslinked with EGS, the PBS-dissolved samples were treated with 1 M hydroxylamine-HCl pH 8.5 for 6 h at 37 °C prior to formaldehyde crosslink reversal.

2.3.6. Protein fractionation by SDS-PAGE for mass spectrometry (MS)

Proteins were fractionated by SDS-PAGE, using precast gels. The run was stopped when the dye front reached ~½ to ¾ of the gel. Gels were rinsed with H_2O, stained with Simply Blue Safe Stain (Invitrogen) for 1 h and destained with H_2O for 1 h. The stained gels typically give a smeary pattern without distinct strong bands.

2.4. Dot-blot analysis to test specific recovery of telomeric DNA in ChIP/QTIP

2.4.1. Reagents

- QIAquick PCR Purification kit (Qiagen).
- Dot-blotting apparatus: e.g. Bio-Dot microfiltration apparatus (Bio-Rad).
- Hybond-N+ membrane (RPN 303B Amersham).
- Stratalinker UV crosslinker (Stratagene).
- Hybridization oven and bottles.
- Church buffer: 0.5 M sodium phosphate buffer pH 7.2, 1 mM EDTA, 7% SDS, 1% BSA.
- Membrane wash buffer: 1× SSC, 0.5% SDS.
- Membrane stripping buffer: 0.1× SSC, 1% SDS.
- Telomeric probe: The radioactive telomeric probe was prepared using RadPrime DNA Labeling (Invitrogen #18428011) of a telomeric DNA template that consisted of a mixture of 1–5 kb long telomeric DNA fragments generated by PCR using DNA self-annealing oligonucleotides $(TTAGGG)_5$ and $(CCCTAA)_5$. For labeling, random primers were annealed to the denatured telomeric DNA template and extended by Klenow fragment in the presence of α^{32}P-dCTP and cold dTTP and dATP thus detecting the telomeric G-rich strand. The labeled probe was purified on a mini Quick Spin DNA Column (Roche). 200 ng of template was used per labeling reaction. The probe was heat-denatured 10 min at 95 °C prior to use.
- Alu-repeat probe: The oligonucleotide probe 5′-GTGATCCGCCC GCCTCGGCCTCCCAAAGTG-3′ was 5′-end-labeled with γ-^{32}P-ATP by T4 polynucleotide kinase, and purified on a mini Quick Spin Oligo Column (Roche).

2.4.2. Procedure

The samples (typically QTIP input and eluates) were treated with crosslink reversal buffer at 65 °C for 7 h to overnight. DNA was purified using spin columns (QIAquick PCR Purification Kit, Qiagen). Alternatively, standard phenol:chloroform extractions were used followed by ethanol precipitation. The DNA was heat-denatured 10 min at 95 °C and blotted onto positively charged nylon membranes (Hybond-N+, Amersham), soaked in 2x SSC. After rinsing with 2x SSC, the DNA was UV-crosslinked to the membrane (Stratalinker, auto-crosslink, 1,200 × 100 μJ). Crosslinked membranes were denatured in 1.5 M NaCl, 0.5 M NaOH for 15 min, followed by neutralization in 0.5 M Tris-HCl pH 7.0, 1 M NaCl for 10 min. Membranes were pre-hybridized in Church buffer for 1 h and incubated overnight with the radiolabeled probes. Hybridized membranes were washed three times for 30 min with 1× SSC, 0.5% SDS. Pre-hybridization, hybridization and washes were performed at 65 °C and 55 °C for telomeric and Alu probes, respectively. Blots were first hybridized and analyzed with the telomeric probe before stripping and reprobing the membrane with the Alu-repeat probe. Membrane stripping was achieved by incubating the membrane three times for 10 min with 0.1× SSC, 1% SDS at 95 °C. Quantification of phosphoimager results allowed determination of the recovery of telomeric DNA and enrichment of telomeric DNA over Alu-repeat DNA.

2.5. Mass spectrometry and data processing

2.5.1. In-gel digestion and LC–MS/MS

Entire gel lanes were cut into pieces, centrifuged and the remaining liquid was discarded. To remove the Coomassie brilliant blue stain and traces of detergents, the gel pieces were washed twice for 20 min in 50% ethanol, 50 mM ammonium bicarbonate (AB, Sigma-Aldrich 09830) and dried down by vacuum centrifugation. Disulfide bridges in proteins were reduced into thiol groups with 10 mM dithioerythritol (DTE, Merck-Millipore 124511) in 50 mM AB at 56 °C for 1 h. The samples were washed and dried as above and the cysteine thiol groups were alkylated with 55 mM iodoacetamide (IAA, Sigma-Aldrich I1149) in 50 mM AB for 45 min at 37 °C in the dark. Alkylation prevents restoration of disulfide bonds thus improving accessibility of proteins for digestion. The alkylated samples were washed and dried again. For rehydration, the gel pieces were incubated for 20 min on ice in a trypsin solution (12.5 ng/μl trypsin Gold (Promega V5280) in 50 mM AB pH 8.4, 10 mM $CaCl_2$). Digestion was continued overnight at 37 °C. The tryptic peptides were extracted twice for 20 min in 70% ethanol, 5% formic acid (Merck-Millipore 100264) with permanent shaking. The supernatants were pooled and dried by vacuum centrifugation. The peptides were re-dissolved in 20 μl 2% acetonitrile (ACN, Fisher Scientific: A/0626/17), 0.1% formic acid for LC–MS/MS injection.

The LC–MS/MS analysis was performed on an Ultimate 3000 RSLC nano system (Dionex/Thermo Fisher Scientific) coupled to an Orbitrap Elite Mass Spectrometer (Thermo Fisher Scientific) piloted with Xcalibur (version 2.1) and Tune (version 2.5.5). The peptide samples were loaded in duplicate onto a pre-column (used for peptide trapping and cleanup; packed in-house; Magic AQ C18; 3 μm-200 Å; 2 cm × 100 μm ID) followed by separation on the analytical column (Nikkyo Technos; Magic AQ C18; 3 μm-100 Å; 15 cm × 75 μm ID). The peptides were separated over a 130-min biphasic gradient ranging from 1.98% ACN, 0.099% FA (aqueous) to 81% ACN, 0.09% FA (organic), at a flow rate of 250 nl/min. The mass spectrometer was operated in a data-dependent acquisition mode with a dynamic exclusion window of 40 s to avoid repeated sequencing of peptides. Each acquisition cycle comprised a single full scan mass spectrum (m/z = 300–1,800) in the Orbitrap (r = 60,000 at m/z = 400), followed by CID (Collision Induced Dissociation) fragmentation on the top 30 most intense precursor ions in the Linear Ion Trap. A threshold of 500 counts was applied to trigger the fragmentation and singly charged ions were excluded. The following source and fragmentation settings were used: capillary voltage 1.9 kV; capillary temperature 240 °C; normalized collision energy 35%; activation Q 0.25; activation time 10 ms.

2.5.2. Data processing

Raw MS data were analyzed with MaxQuant version 1.2.2.5 with the integrated peptide search engine Andromeda (freely available at www.maxquant.org [49,50]). Searches were performed against a human Uniprot database, using arginine (R10) and lysine (K8) as heavy labels (multiplicity of 2). To assess the likelihood of false positive identifications, the sequence list was complemented with known common contaminant sequences and reversed sequences (the amino acids of original protein sequences were organized in reverse order). The searches were performed at precursor mass accuracy of 7 ppm and MS/MS accuracy of 0.5 Da. The enzyme was set to trypsin with up to two missed cleavages. Since reduction and alkylation of cysteine residues result in carbamidomethyl modifications that increase the mass of cysteines by 57 Da, carbamidomethylation was set as a fixed modification.

Oxidation of methionine and acetylation of the protein N terminus were set as variable modifications. The minimal peptide length was set to six amino acids and at least two (unique+razor) peptides were required for protein identification. A cut-off was set to 0.1 for posterior error probability, which is the probability of a peptide to be a false hit considering identification score and peptide length. Only identifications with false discovery rates (FDR) <0.01 were accepted at both the peptide and protein levels. When multiple labeled peptides were observed in an experiment, MaxQuant calculated 'heavy' to 'light' ratios for individual protein groups. The ratios were calculated using unique and razor peptides. A minimum of two SILAC ratio counts was required for quantification of a protein group. The mass spectrometry proteomics data discussed in this manuscript were generated as described previously [42] and deposited to the ProteomeXchange Consortium (http://proteomecentral.proteomexchange.org) via the PRIDE partner repository with the dataset identifier PXD000243 (Approach A files).

2.5.3. Data analysis

The downstream analysis was done using the Perseus software version 1.5.3.2 which is freely available at http://www.coxdocs.org/. To clean and filter the data, protein groups only identified by a modification site, and proteins matching the reversed and contaminant sequences were removed from the dataset. To compare protein recovery in telomere specific anti-TRF1+2 IP and control IgG IP, we calculated the so-called TRF1+2/IgG enrichment using corresponding iBAQ values. iBAQ (intensity-based absolute quantification) represents the sum of peak intensities of all peptides (heavy + light) matching to a specific protein divided by the number of theoretically observable peptides. iBAQ is thus an abundance measure normalized to protein length and sequence. The mean iBAQ values from two replicates (forward and reverse experiments) were $\log_2$ transformed before calculating the TRF1+2/IgG ratio. Statistically significant outliers (i.e. proteins enriched in anti-TRF1+2 IP over IgG IP) were calculated using a Significance A left-sided test (p-value <0.05). However, manual inspection of each dataset was necessary to set an appropriate threshold value. The known telomeric proteins should pass the threshold, whereas common contaminating proteins, such as cytoskeletal, ribosomal and abundant metabolic proteins should be eliminated. The cut-off was set based on the achieved purification factor, and the relative costs of false positives and false negatives.

To identify proteins that were enriched at telomeres in the two tested conditions (in our case, long telomeres versus short telomeres), significant SILAC ratios were determined separately for the two replicates using Significance B two-sided tests, using the default Benjamini-Hochberg multiple hypothesis testing correction and FDR with a threshold of 0.05. In contrast to Significance A, Significance B is intensity-dependent and compensates for the bias of highly abundant proteins being more accurately quantified than low abundant proteins. Definition of TRF-enriched proteins and the up-regulated and down-regulated subsets allows annotation enrichment analysis, such as the Fisher exact test to see if the subset is enriched in (or depleted of) some Gene Ontology (GO) terms [51] or KEGG (Kyoto Encyclopedia of Genes and Genomes) pathways [52]. This is a fast test to verify that the TRF-enriched proteins are predominantly nuclear/chromatin-associated and functionally relevant, and may reveal unexpected shared functions between the differentially regulated proteins.

To visually examine the data in Perseus, one can construct a scatter plot with SILAC ratios from forward and reverse replicates of the label swap experiment plotted against each other. Only proteins identified and quantified in both replicates will be displayed, directing the attention to high-confidence hits. In addition, the proteins can be color-coded according to their TRF1+2/IgG enrichment or their affiliation with a certain GO term. The integration of SILAC ratios, TRF1+2/IgG enrichment scores and categorical annotation facilitates the selection of candidate proteins for further investigation.

3. Results

3.1. Workflow for the quantitative analysis of telomeric proteomes by QTIP

QTIP allows comparison of telomeric protein composition between cells with different telomeric states. It combines three well-established techniques: SILAC labeling, chromatin immunoprecipitation, and mass spectrometry. The protocol consists of the following steps (Fig. 1A). First, the polypeptides of the two cell populations are differentially labeled using SILAC, and mixed in a 1:1 ratio. If telomere lengths between the cells to be compared differ, mixing ratios may be adjusted in order to start with equal amounts of telomeric chromatin. The cells are treated with formaldehyde (or formaldehyde in combination with ethylene glycol bis(succinimidyl succinate) (EGS)), resulting in covalent crosslinking of nucleoprotein complexes. Subsequently, chromatin is extracted and sheared into shorter fragments by sonication. This preparation is subjected to immunoprecipitation using affinity-purified antibodies against the abundant telomeric proteins TRF1 and TRF2 in order to isolate telomeric chromatin. Generally, the yield of chromatin in a locus-specific ChIP is quite low, but the presence of TRF1 and TRF2 throughout telomeric repeat sequences and their presence at each chromosome end facilitate the isolation of telomeric chromatin. Parallel immunoprecipitation using non-specific IgG is performed on the same extract to identify contaminants that bind unspecifically to the beads and that are released together with the proteins of interest upon elution. The proteins isolated with anti-TRF1/2 and IgG antibodies are both resolved using SDS-PAGE prior to analysis by LC–MS/MS. Thanks to differential SILAC labeling, proteins coming from the two cell populations can be distinguished, and their relative abundance determined.

3.2. Generation and characterization of anti-TRF1 and anti-TRF2 specific antibodies

One of the most critical determinants of a successful ChIP-based approach is the antibody. ChIP antibodies should capture the target protein with high efficiency and highest possible specificity. Chemical crosslinking and sonication may lead to epitope masking or destruction. Epitope masking can be more problematic for monoclonal antibodies or peptide antibodies because they usually recognize only a single epitope. Therefore, polyclonal antibodies generated against intact native proteins, fusion proteins, or large protein fragments are preferred. We used custom-manufactured rabbit polyclonal antibodies raised and affinity-purified against full-length TRF1 and TRF2 recombinant proteins (Fig. 1B). Every batch of serum and purified antibodies is properly characterized and its suitability for ChIP is assessed. The antibodies are also tested for off-target binding using positive and negative controls. Usually, the crude serum is first tested for antigen recognition by immunoblotting of cell lysates. The intensity of the correct band is reduced upon depletion of the target protein by RNA interference. To further evaluate the capacity of antisera to capture endogenous TRF1 and TRF2 and to test their specificity, we perform small-scale ChIP experiments. Well-performing sera are selected for affinity purification of anti-TRF1 and anti-TRF2 specific antibodies. The purified antibodies are quantified, and titration experiments are performed to determine the antibody concentration that gives a maximum yield of telomeric DNA, while minimizing precipitation of nonspecific DNA (Fig. 2A and B). As a control for

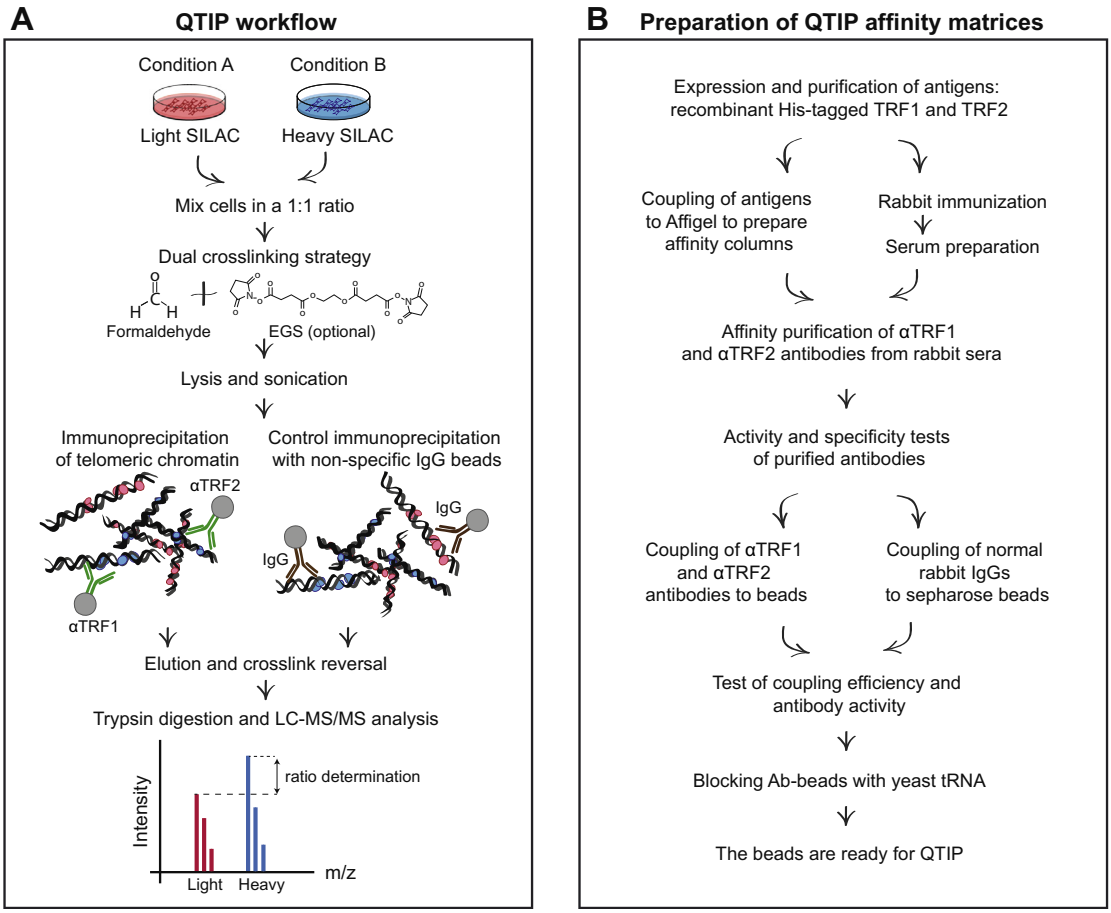

Fig. 1. Outline of the QTIP procedure. (A) Proteins in the two cell populations having different telomeric states are metabolically labeled by culturing with light or heavy amino acids to allow discrimination of respective proteomes based on peptide mass differences. The cells from conditions A and B are harvested and mixed in a 1:1 ratio, chemically crosslinked and subjected to lysis, chromatin enrichment and sonication. The sonicated chromatin is split into two IP reactions: telomeric chromatin is purified using antibodies against telomeric proteins TRF1 and TRF2, while the IP with normal rabbit IgGs is used as a control for nonspecific binding to the affinity matrix. Following crosslink reversal, the immunoprecipitated proteins are resolved by SDS-PAGE. Each gel lane is cut into 8–10 slices that are subjected to protein digestion and analysis by LC–MS/MS. The relative intensities of MS signals for light and heavy peptides correspond to the relative abundance of a peptide, and the corresponding protein, in conditions A and B. (B) Workflow for the preparation of QTIP affinity matrices. Recombinant human TRF1 and TRF2 proteins serve first as antigens for rabbit immunization and later as baits for affinity purification of anti-TRF1 and anti-TRF2 specific antibodies from rabbit sera. The purified antibodies are quantified and tested for activity and specificity. Based on titration, a saturating amount of anti-TRF1 and anti-TRF2 antibodies, and an equivalent amount of normal rabbit IgGs is covalently coupled to Protein G Sepharose beads. Prior to use, the beads are blocked with yeast tRNA to reduce nonspecific binding to affinity resin.

nonspecific binding, we assess the capture of Alu-repeat DNA that is not associated with TRF1 and TRF2. For QTIP, we select anti-TRF1 and anti-TRF2 antibody preparations that recover at least 20% and 8% of telomeric DNA in small-scale experiments, respectively. The fold enrichment of recovered telomeric DNA over contaminating Alu-repeat DNA should exceed 150 and 80, for anti-TRF1 and anti-TRF2 antibodies respectively. Reaction upscaling typically leads to a mild decrease in recovery, but a significant increase in specificity. When anti-TRF1 and anti-TRF2 antibodies are combined in single QTIP experiments, recovery values are in the range of 5–20%, with telomeric/Alu repeat DNA ratios of 250 to over 1,500.

3.3. SILAC labeling of cell cultures

To ensure high quantitative accuracy in comparative proteomic experiments, the two samples should be combined at a very early step. This prevents the detection of artifacts caused by differential handling of samples. For this reason, the QTIP technique takes advantage of SILAC labeling of cell cultures that unlike chemical derivatization methods enables the two proteomes to be combined upstream of protein extraction, at the intact cell level.

Using SILAC, cells are metabolically labeled through growth in medium lacking a standard essential amino acid but supplemented with an isotope-labeled form of that amino acid. For example, the so-called ‘heavy’ amino acids have naturally ‘light’ ^{12}C carbon and ^{14}N nitrogen substituted with the heavy isotopes ^{13}C and ^{15}N. The heavy amino acids are incorporated into newly synthesized proteins, labeling the cellular proteome within a few cell doublings to near completion. By using heavy arginine (R10) and lysine (K8), proteins are labeled specifically at sites of trypsin cleavage, which is convenient for subsequent analysis of tryptic peptides by mass spectrometry. When ‘light’ and ‘heavy’ cell populations are mixed for the experiment, peptides resulting from trypsin digests are detected by mass spectrometry in form of ion pairs (doublets), and their ratios reflect the relative changes in protein abundance between the light and the heavy condition.

When applying QTIP to a new cell line, the cell culture medium composition must be optimized for the incorporation of labeled amino acids and cell growth (Fig. 3). SILAC amino acids have no known adverse effects on cell growth and metabolism but the dialyzed fetal bovine serum may lack some small-molecule factors important for cell growth. Upon adapting a new cell line to SILAC medium, the growth kinetics must be monitored. Lysine and

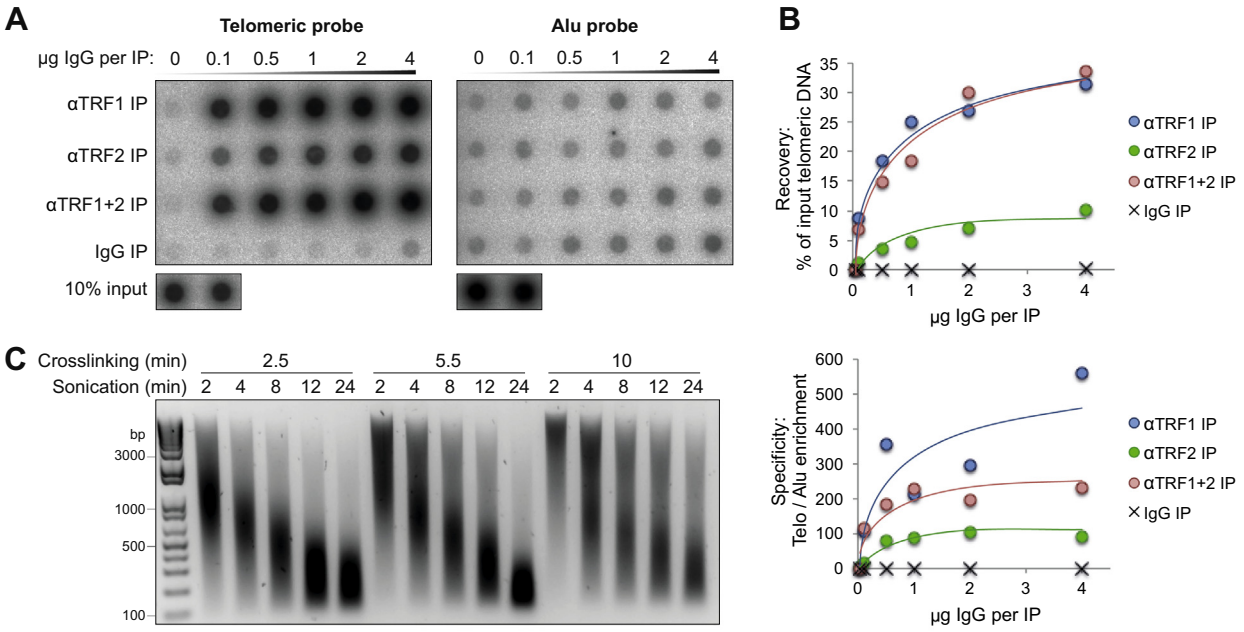

Fig. 2. Optimization of experimental parameters for QTIP. (A and B) Titration of affinity purified anti-TRF1 and anti-TRF2 antibodies for telomeric ChIP. Telomeric chromatin was immunoprecipitated with increasing amounts of antibody (0–4 µg of total IgGs per 2×10^6 cells in ~600 µl). The immunoprecipitated DNA was analyzed on dot-blots by hybridization with a specific telomeric probe and a control Alu-repeat probe. The amounts of precipitated telomeric DNA were quantified and compared to the telomeric DNA in the soluble chromatin fraction (input). Fold enrichment of precipitated telomeric DNA compared to precipitated Alu-repeat DNA depends on antibody specificity. (C) Effects of various crosslinking and sonication times on chromatin fragment length. Immortalized human fibroblasts were crosslinked in solution with 1% formaldehyde for the indicated times at 24 °C. Chromatin was enriched and sonicated using Covaris E220 for the indicated times at 4 °C. Following crosslink removal, the DNA was extracted and analyzed on a 1% agarose gel. Fragments above 1 kb are considered under-sonicated.

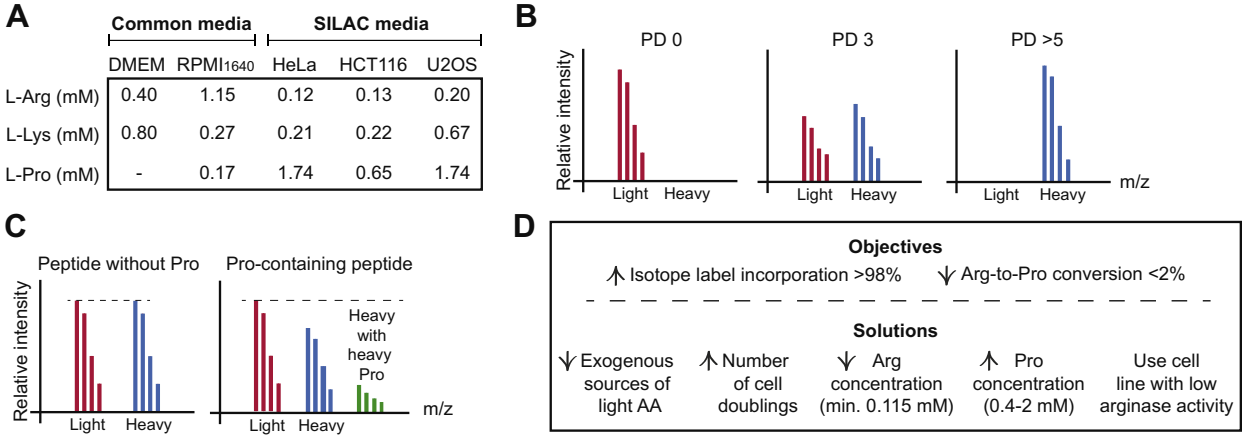

Fig. 3. SILAC for quantitative proteomics. (A) Concentrations of amino acids used in growth media for adherent (DMEM) and suspension (RPMI-1640) cells, and optimized concentrations for selected cell lines. (B) Expected behavior of SILAC peptides during a time course experiment for isotope label incorporation. (C) Effects of metabolic conversion of isotope-labeled arginine to proline. Theoretical mass spectra of peptide ions (with and without proline) from a 1:1 mixture of light-labeled and heavy-labeled samples are shown. For a peptide without proline, light and heavy peptide ions show the expected 1:1 ratio, while the peak intensity of light proline-containing peptides approximately equals the combined intensities of the corresponding heavy peptides and the heavy peptides that contain heavy proline. (D) Overview of SILAC labeling guidelines.

arginine concentrations are titrated and light proline may be added. SILAC labeling is measured over time to determine the time that is required for maximal incorporation of heavy Arg and Lys (Fig. 3A and B). Since arginine and lysine may have different labeling efficiencies, the calculation should be performed separately for arginine- and for lysine-containing peptides. Since some cell lines metabolically convert arginine to proline (Fig. 3C) and *vice versa*, an optimal balance between arginine and proline concentrations has to be established. For accurate quantification, >98% incorporation rate of heavy amino acids is required. The arginine-to-proline conversion rate should be <2–3%. Practical guidelines for the design of successful SILAC labeling experiments are given in 2.2 (Fig. 3D).

In this manuscript, we present QTIP comparisons of two cell states. However, it is possible to compare three conditions in a single experiment using a triple SILAC labeling strategy. This requires growing cells in light (K0R0), medium (K4R6), and heavy (K8R10) growth medium. Each peptide identified by the mass spectrometer will appear as a triplet and the ratio between the three peptide peaks will indicate the relative abundance of a protein at telomeres

in the three conditions. In case that SILAC labeling is impossible, label-free quantification provides an alternative route to determine the relative amounts of proteins in two or more samples. This quantification can be based on the precursor signal intensity or on spectral counting, which relies on the number of MS/MS spectra acquired for a certain protein. At least three replicates are required for accurate quantification. Finally, proteins of different samples can be chemically labeled post lysis with different isotopes [53].

3.4. Optimization of QTIP assay conditions

For each cell line, we first perform time-course experiments to test cross-linking and sonication conditions (Fig. 2C). Live cells are fixed to generate protein-protein and protein-nucleic acid cross-links between molecules in close proximity on the chromatin *in vivo*. This decreases the possibility that complexes rearrange during processing, and allows stringent washes to remove non-specific interactors. The extent of cross-linking is dependent on the identity of the cross-linking reagent, its concentration and the duration and temperature of incubation. Insufficient cross-linking results in losses of interactions, whereas excessive cross-linking can interfere with sonication and may lead to epitope masking or aggregation. The most commonly used cross-linker formaldehyde reacts with primary amines on amino acids and DNA and RNA bases, forming a covalent adduct between two primary amines that are in close proximity (⩽2 Å). Formaldehyde cross-linking is particularly efficient for proteins such as histones that form direct contacts with DNA and possess long N-terminal tails composed mainly of basic amino-acid residues that readily react with formaldehyde. However, to crosslink transient interactors, larger multiprotein complexes and proteins that are more distant from the core chromatin, longer cross-linking times should be employed. The co-immunoprecipitation efficiency of these proteins may be improved when in addition to formaldehyde, a

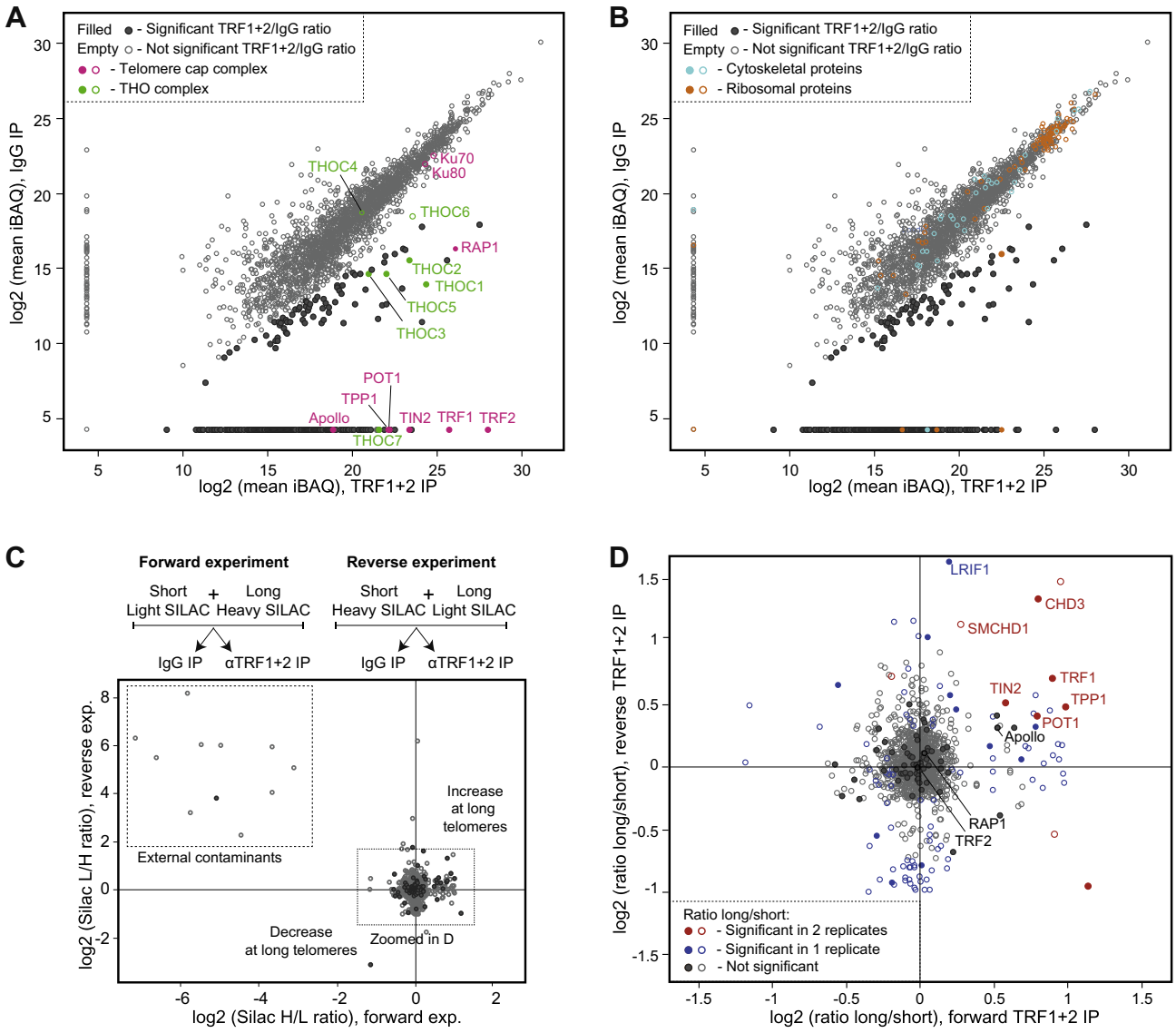

Fig. 4. QTIP identifies novel telomeric components and quantifies differences in protein composition of short and long telomeres. (A) Scatter plot showing an example of enrichment of known (pink) and novel (green) telomeric proteins in a QTIP experiment performed on isogenic HeLa cell lines with short and long telomeres. 324 out of 2,738 proteins from 2 biological replicates were classified as telomere-enriched based on the TRF1+2/IgG ratio of Log_2 transformed mean iBAQ values (Significance A, left side, p-value < 0.05). (B) The majority of abundant background proteins, such as ribosomal (brown, GO:0003735) and cytoskeletal (cyan, GO:0005200) proteins, was isolated in both anti-TRF1+2 and IgG IP, and thus was removed from the candidate list. (C and D) The label-swap experimental approach discriminates false-positives from true hits that show reverse correlation between the SILAC ratios in forward and reverse experiments. The significant outliers are color-coded in D (Significance B, both sides, Benjamini-Hochberg FDR, p-value <0.05). The data are from [42].

protein-protein crosslinking agent is included [54,55]. For QTIP we obtained good results when combining formaldehyde with EGS, an amine-reactive cross-linker with a 12-atom spacer arm of 16 Å, which can be cleaved by treatment with hydroxylamine at pH 8.5. Crosslinking with 1% formaldehyde and 2 mM EGS for 10–30 min at 25 °C to 30 °C gave satisfactory results.

Efficient sonication of chromatin to small particles with DNA fragments of 0.2–0.6 kb increases chromatin solubility and improves the separation of telomeric from subtelomeric chromatin. However, over-sonication may disrupt cross-linked nucleoprotein complexes and cause protein damage both of which reduce ChIP efficiency. Therefore, several cross-linking and sonication conditions must be tested in time-course experiments at a small scale in which recovery and specificity are measured. Conditions that give the highest signal-to-noise ratio and acceptable recovery are chosen for pilot QTIP experiments performed at large scale but without SILAC labeling. These experiments allow determining the cell number that is required for good MS identification of telomeric proteins. However, the sensitivity of the actual QTIP experiments will be lower owing to the increased sample complexity (SILAC doubles the number of peptides in the mixture).

QTIP immunoprecipitation efficiencies and specificity vary among cell lines possibly due to differences in telomere length and abundance and/or accessibility of TRF1 and TRF2. We start with chromatin-enriched fractions, removing the excess of cytosolic proteins. Nonspecific binding to the affinity matrix is reduced by pre-blocking the bead surface with yeast tRNA. Strong matrix binding proteins are removed from the sonicated chromatin during a pre-clearing step in which the sonicated chromatin is incubated with beads in the absence of antibodies. Presence of high salt and detergents during the purification procedure also reduces the background. On the other hand, detergents can be the source of PEG contaminations that perturb MS analysis. SDS-PAGE prior to MS analysis overcomes this problem. Remaining contaminants are identified by performing parallel immunoprecipitations with normal rabbit IgGs.

3.5. Applications of QTIP

We determined the telomeric proteome of Hela cells by QTIP demonstrating that this method provides an *in vivo* snapshot of telomeric chromatin [42]. A parallel experiment using nonspecific IgGs facilitated blacklisting of background binders (Fig. 4A and B). QTIP identified all six shelterin subunits (TRF1, TRF2, Rap1, TPP1, TIN2, POT1) and many of the known telomere associated factors (e.g. Apollo, Mre11, Nbs1 Rad50, Gar1). Among the newly identified proteins, we discovered the THO complex at telomeres, and later its roles in counteracting telomeric DNA:RNA hybrids in yeast [43]. We also detected by QTIP the lysine demethylase LSD1 at telomeres and characterized its functions upon TRF2 depletion [31]. Comparison of telomere protein composition of wild type HeLa cells (average telomere length of 10 kb) and HeLa cells with overelongated telomeres (average telomere length of 30 kb) (Fig. 4C and D [42]), revealed that longer telomeres contain increased absolute amounts of the shelterin components TRF1, TIN2, TPP1 and POT1. However, TRF2 and RAP1 were not increased in HeLa cells with long telomeres indicating different modes of regulation for TRF1 and TRF2. Moreover, we identified LRIF1 and SMCHD1, as-yet-unknown telomeric factors that preferentially associated with long telomeres. These factors are crucial for compaction of the inactive X chromosome in females and we therefore speculate that they might also have structural roles in telomeric chromatin. The QTIP protocol can be adapted to various human cell lines and we already implemented it to HEK293, U2OS, HCT116 as well as primary fibroblasts. In addition, we successfully performed QTIP experiments with antibodies against POT1 and TPP1, which are thought to be enriched near the telomeric 3'overhang thus preferentially enriching for chromosome end binding proteins (unpublished).

The number of telomeropathies with ambiguous and complex etiology has been increasing continuously over the last decade. QTIP should be instrumental to reveal the molecular defects at telomeres in these patients by comparing patient-derived and healthy control cells. Alternatively, patient mutations can by introduced by genome editing in cell lines of choice. Likewise, QTIP can give clues about telomere protein functions by studying the consequences of their depletion using established knockdown or knockout technologies. For example, we induced the depletion of TRF2 or POT1 and thereby characterized the telomeric DNA damage response [42]. Finally, it should be possible to identify by QTIP the changes that may occur in telomeric chromatin during other physiological and pathological conditions such as the cell cycle, during cell differentiation and reprogramming.

4. Conclusions

We expect that QTIP will be instrumental to obtain crucial novel insights into the roles of telomeres in normal cells and disease. The comprehensive analysis of telomeric chromatin should identify additional critical factors for telomere function and it should become possible to identify specific telomere signatures for normal development, aging, cancer and telomere diseases. QTIP has significant advantages over the previously employed *in vitro* methods of identifying telomeric proteins. A method termed PICh, in which telomeres are partially denatured and affinity purified via antisense hybridization, was described by Déjardin and Kingston [56]. In both QTIP and PICh, telomeric chromatin is cross-linked *in vivo* and subsequently purified. In contrast to QTIP, PICh includes an RNase step, which may lead to the loss of TERRA-dependent telomeric factors and PICh requires higher cell numbers than QTIP. QTIP and PICh also differ with regard to crosslinking conditions. Both methods represent a significant advance over attempts to study telomeric chromatin upon reconstitution and promise to provide complementary insight into the telomeric proteome.

Acknowledgements

We thank L. Grolimund and E. Aeby for QTIP development, labmembers for discussion and F. Armand, R. Hamelin, D. Chiappe and M. Moniatte for mass spectrometry analysis. Research in J.L.'s laboratory was supported by the Swiss National Science Foundation (SNSF), the SNSF funded NCCR RNA and disease network, an Initial Training Network (ITN) grant (CodeAge) from the European Commission's Seventh Framework Programme [grant agreement number 316354], the Swiss Cancer League and EPFL.

References

[1] T. de Lange, How telomeres solve the end-protection problem, Science 326 (5955) (2009) 948–952.
[2] P. Baumann, T. Cech, Pot1, the putative telomere end-binding protein in fission yeast and humans, Science 292 (2001) 1171–1175.
[3] A. Sfeir, T. de Lange, Removal of shelterin reveals the telomere end-protection problem, Science 336 (6081) (2012) 593–597.
[4] A. Sfeir, S.T. Kosiyatrakul, D. Hockemeyer, S.L. MacRae, J. Karlseder, C.L. Schildkraut, T. de Lange, Mammalian telomeres resemble fragile sites and require TRF1 for efficient replication, Cell 138 (1) (2009) 90–103.
[5] K.M. Miller, O. Rog, J.P. Cooper, Semi-conservative DNA replication through telomeres requires Taz1, Nature 440 (7085) (2006) 824–828.
[6] E. Abreu, E. Aritonovska, P. Reichenbach, G. Cristofari, B. Culp, R.M. Terns, J. Lingner, M.P. Terns, TIN2-tethered TPP1 recruits human telomerase to telomeres in vivo, Mol. Cell. Biol. 30 (12) (2010) 2971–2982.
[7] F.L. Zhong, L.F. Batista, A. Freund, M.F. Pech, A.S. Venteicher, S.E. Artandi, TPP1 OB-Fold domain controls telomere maintenance by recruiting telomerase to chromosome ends, Cell 150 (3) (2012) 481–494.

[8] J. Nandakumar, C.F. Bell, I. Weidenfeld, A.J. Zaug, L.A. Leinwand, T.R. Cech, The TEL patch of telomere protein TPP1 mediates telomerase recruitment and processivity, Nature 492 (7428) (2012) 285–289.
[9] A.N. Sexton, S.G. Regalado, C.S. Lai, G.J. Cost, C.M. O'Neil, F.D. Urnov, P.D. Gregory, R. Jaenisch, K. Collins, D. Hockemeyer, Genetic and molecular identification of three human TPP1 functions in telomerase action: recruitment, activation, and homeostasis set point regulation, Genes Dev. 28 (17) (2014) 1885–1899.
[10] H. Kocak, B.J. Ballew, K. Bisht, R. Eggebeen, B.D. Hicks, S. Suman, A. O'Neil, N. Giri, I. Maillard, B.P. Alter, C.E. Keegan, J. Nandakumar, S.A. Savage, Hoyeraal-Hreidarsson syndrome caused by a germline mutation in the TEL patch of the telomere protein TPP1, Genes Dev. 28 (19) (2014) 2090–2102.
[11] S.A. Savage, N. Giri, G.M. Baerlocher, N. Orr, P.M. Lansdorp, B.P. Alter, TINF2, a component of the shelterin telomere protection complex, is mutated in dyskeratosis congenita, Am. J. Hum. Genet. 82 (2) (2008) 501–509.
[12] A.J. Walne, T. Vulliamy, R. Beswick, M. Kirwan, I. Dokal, TINF2 mutations result in very short telomeres: analysis of a large cohort of patients with dyskeratosis congenita and related bone marrow failure syndromes, Blood 112 (9) (2008) 3594–3600.
[13] H. Takai, E. Jenkinson, S. Kabir, R. Babul-Hirji, N. Najm-Tehrani, D.A. Chitayat, Y. J. Crow, T. de Lange, A POT1 mutation implicates defective telomere end fill-in and telomere truncations in Coats plus, Genes Dev. 30 (7) (2016) 812–826.
[14] Y. Guo, M. Kartawinata, J. Li, H.A. Pickett, J. Teo, T. Kilo, P.M. Barbaro, B. Keating, Y. Chen, L. Tian, A. Al-Odaib, R.R. Reddel, J. Christodoulou, X. Xu, H. Hakonarson, T.M. Bryan, Inherited bone marrow failure associated with germline mutation of ACD, the gene encoding telomere protein TPP1, Blood 124 (18) (2014) 2767–2774.
[15] A.J. Ramsay, V. Quesada, M. Foronda, L. Conde, A. Martinez-Trillos, N. Villamor, D. Rodriguez, A. Kwarciak, C. Garabaya, M. Gallardo, M. Lopez-Guerra, A. Lopez-Guillermo, X.S. Puente, M.A. Blasco, E. Campo, C. Lopez-Otin, POT1 mutations cause telomere dysfunction in chronic lymphocytic leukemia, Nat. Genet. 45 (5) (2013) 526–530.
[16] A.M. Pinzaru, R.A. Hom, A. Beal, A.F. Phillips, E. Ni, T. Cardozo, N. Nair, J. Choi, D. S. Wuttke, A. Sfeir, E.L. Denchi, Telomere replication stress induced by POT1 inactivation accelerates tumorigenesis, Cell Rep. 15 (10) (2016) 2170–2184.
[17] Y. Miyake, M. Nakamura, A. Nabetani, S. Shimamura, M. Tamura, S. Yonehara, M. Saito, F. Ishikawa, RPA-like mammalian Ctc1-Stn1-Ten1 complex binds to single-stranded DNA and protects telomeres independently of the Pot1 pathway, Mol. Cell 36 (2) (2009) 193–206.
[18] Y.V. Surovtseva, D. Churikov, K.A. Boltz, X. Song, J.C. Lamb, R. Warrington, K. Leehy, M. Heacock, C.M. Price, D.E. Shippen, Conserved telomere maintenance component 1 interacts with STN1 and maintains chromosome ends in higher eukaryotes, Mol. Cell 36 (2) (2009) 207–218.
[19] P. Wu, H. Takai, T. de Lange, Telomeric 3' overhangs derive from resection by Exo1 and Apollo and Fill-In by POT1b-associated CST, Cell 150 (1) (2012) 39–52.
[20] P. Gu, J.N. Min, Y. Wang, C. Huang, T. Peng, W. Chai, S. Chang, CTC1 deletion results in defective telomere replication, leading to catastrophic telomere loss and stem cell exhaustion, EMBO J. 31 (10) (2012) 2309–2321.
[21] J.A. Stewart, F. Wang, M.F. Chaiken, C. Kasbek, P.D. Chastain 2nd, W.E. Wright, C.M. Price, Human CST promotes telomere duplex replication and general replication restart after fork stalling, EMBO J. 31 (17) (2012) 3537–3549.
[22] L.Y. Chen, S. Redon, J. Lingner, The human CST complex is a terminator of telomerase activity, Nature 488 (7412) (2012) 540–544.
[23] B.H. Anderson, P.R. Kasher, J. Mayer, M. Szynkiewicz, E.M. Jenkinson, S.S. Bhaskar, J.E. Urquhart, S.B. Daly, J.E. Dickerson, J. O'Sullivan, E.O. Leibundgut, J. Muter, G.M. Abdel-Salem, R. Babul-Hirji, P. Baxter, A. Berger, L. Bonafe, J.E. Brunstom-Hernandez, J.A. Buckard, D. Chitayat, W.K. Chong, D.M. Cordelli, P. Ferreira, J. Fluss, E.H. Forrest, E. Franzoni, C. Garone, S.R. Hammans, G. Houge, I. Hughes, S. Jacquemont, P.Y. Jeannet, R.J. Jefferson, R. Kumar, G. Kutschke, S. Lundberg, C.M. Lourenco, R. Mehta, S. Naidu, K.K. Nischal, L. Nunes, K. Ounap, M. Philippart, P. Prabhakar, S.R. Risen, R. Schiffmann, C. Soh, J.B. Stephenson, H. Stewart, J. Stone, J.L. Tolmie, M.S. van der Knaap, J.P. Vieira, C.N. Vilain, E.L. Wakeling, V. Wermenbol, A. Whitney, S.C. Lovell, S. Meyer, J.H. Livingston, G. M. Baerlocher, G.C. Black, G.I. Rice, Y.J. Crow, Mutations in CTC1, encoding conserved telomere maintenance component 1, cause Coats plus, Nat. Genet. 44 (3) (2012) 338–342.
[24] R.B. Keller, K.E. Gagne, G.N. Usmani, G.K. Asdourian, D.A. Williams, I. Hofmann, S. Agarwal, CTC1 mutations in a patient with dyskeratosis congenita, Pediatr. Blood Cancer 59 (2) (2012) 311–314.
[25] A.J. Walne, T. Bhagat, M. Kirwan, C. Gitiaux, I. Desguerre, N. Leonard, E. Nogales, T. Vulliamy, I.S. Dokal, Mutations in the telomere capping complex in bone marrow failure and related syndromes, Haematologica 98 (3) (2013) 334–338.
[26] A. Polvi, T. Linnankivi, T. Kivela, R. Herva, J.P. Keating, O. Makitie, D. Pareyson, L. Vainionpaa, J. Lahtinen, I. Hovatta, H. Pihko, A.E. Lehesjoki, Mutations in CTC1, encoding the CTS telomere maintenance complex component 1, cause cerebroretinal microangiopathy with calcifications and cysts, Am. J. Hum. Genet. 90 (3) (2012) 540–549.
[27] C.M. Azzalin, P. Reichenbach, L. Khoriauli, E. Giulotto, J. Lingner, Telomeric repeat containing RNA and RNA surveillance factors at mammalian chromosome ends, Science 318 (5851) (2007) 798–801.
[28] C.M. Azzalin, J. Lingner, Telomere functions grounding on TERRA firma, Trends Cell Biol. 25 (1) (2015) 29–36.
[29] S. Schoeftner, M.A. Blasco, Developmentally regulated transcription of mammalian telomeres by DNA-dependent RNA polymerase II, Nat. Cell Biol. 10 (2) (2008) 228–236.
[30] A. Porro, S. Feuerhahn, J. Delafontaine, H. Riethman, J. Rougemont, J. Lingner, Functional characterization of the TERRA transcriptome at damaged telomeres, Nat. Commun. 5 (2014) 5379.
[31] A. Porro, S. Feuerhahn, J. Lingner, TERRA-reinforced association of LSD1 with MRE11 promotes processing of uncapped telomeres, Cell Rep. 6 (4) (2014) 765–776.
[32] R.L. Flynn, R.C. Centore, R.J. O'Sullivan, R. Rai, A. Tse, Z. Songyang, S. Chang, J. Karlseder, L. Zou, TERRA and hnRNPA1 orchestrate an RPA-to-POT1 switch on telomeric single-stranded DNA, Nature 471 (7339) (2011) 532–536.
[33] S. Redon, P. Reichenbach, J. Lingner, The non-coding RNA TERRA is a natural ligand and direct inhibitor of human telomerase, Nucleic Acids Res. 38 (17) (2010) 5797–5806.
[34] V. Pfeiffer, J. Lingner, TERRA promotes telomere shortening through exonuclease 1-mediated resection of chromosome ends, PLoS Genet. 8 (6) (2012) e1002747.
[35] S. Yehezkel, Y. Segev, E. Viegas-Pequignot, K. Skorecki, S. Selig, Hypomethylation of subtelomeric regions in ICF syndrome is associated with abnormally short telomeres and enhanced transcription from telomeric regions, Hum. Mol. Genet. 17 (18) (2008) 2776–2789.
[36] K. Paeschke, J.A. Capra, V.A. Zakian, DNA replication through G-quadruplex motifs is promoted by the *Saccharomyces cerevisiae* Pif1 DNA helicase, Cell 145 (5) (2011) 678–691.
[37] J.B. Vannier, V. Pavicic-Kaltenbrunner, M.I. Petalcorin, H. Ding, S.J. Boulton, RTEL1 dismantles T loops and counteracts telomeric G4-DNA to maintain telomere integrity, Cell 149 (4) (2012) 795–806.
[38] L. Crabbe, R.E. Verdun, C.I. Haggblom, J. Karlseder, Defective telomere lagging strand synthesis in cells lacking WRN helicase activity, Science 306 (5703) (2004) 1951–1953.
[39] H. Ding, M. Schertzer, X. Wu, M. Gertsenstein, S. Selig, M. Kammori, R. Pourvali, S. Poon, I. Vulto, E. Chavez, P.P. Tam, A. Nagy, P.M. Lansdorp, Regulation of murine telomere length by Rtel: an essential gene encoding a helicase-like protein, Cell 117 (7) (2004) 873–886.
[40] G. Sarek, J.B. Vannier, S. Panier, J.H. Petrini, S.J. Boulton, TRF2 recruits RTEL1 to telomeres in S phase to promote t-loop unwinding, Mol. Cell 57 (4) (2015) 622–635.
[41] J.D. Griffith, L. Comeau, S. Rosenfield, R.M. Stansel, A. Bianchi, H. Moss, T. de Lange, Mammalian telomeres end in a large duplex loop, Cell 97 (4) (1999) 503–514.
[42] L. Grolimund, E. Aeby, R. Hamelin, F. Armand, D. Chiappe, M. Moniatte, J. Lingner, A quantitative telomeric chromatin isolation protocol identifies different telomeric states, Nat. Commun. 4 (2013) 2848.
[43] V. Pfeiffer, J. Crittin, L. Grolimund, J. Lingner, The THO complex component Thp2 counteracts telomeric R-loops and telomere shortening, EMBO J. 32 (21) (2013) 2861–2871.
[44] W.C. Hahn, S.K. Dessain, M.W. Brooks, J.E. King, B. Elenbaas, D.M. Sabatini, J.A. DeCaprio, R.A. Weinberg, Enumeration of the simian virus 40 early region elements necessary for human cell transformation, Mol. Cell. Biol. 22 (7) (2002) 2111–2123.
[45] A.L. Ducrest, M. Amacker, Y.D. Mathieu, A.P. Cuthbert, D.A. Trott, R.F. Newbold, M. Nabholz, J. Lingner, Regulation of human telomerase activity: repression by normal chromosome 3 abolishes nuclear telomerase reverse transcriptase transcripts but does not affect c-Myc activity, Cancer Res. 61 (20) (2001) 7594–7602.
[46] G. Cristofari, J. Lingner, Telomere length homeostasis requires that telomerase levels are limiting, EMBO J. 25 (3) (2006) 565–574.
[47] S.E. Ong, B. Blagoev, I. Kratchmarova, D.B. Kristensen, H. Steen, A. Pandey, M. Mann, Stable isotope labeling by amino acids in cell culture, SILAC, as a simple and accurate approach to expression proteomics, Mol. Cell Proteomics 1 (5) (2002) 376–386.
[48] S.C. Bendall, C. Hughes, M.H. Stewart, B. Doble, M. Bhatia, G.A. Lajoie, Prevention of amino acid conversion in SILAC experiments with embryonic stem cells, Mol. Cell. Proteomics 7 (9) (2008) 1587–1597.
[49] J. Cox, M. Mann, MaxQuant enables high peptide identification rates, individualized p.p.b.-range mass accuracies and proteome-wide protein quantification, Nat. Biotechnol. 26 (12) (2008) 1367–1372.
[50] J. Cox, N. Neuhauser, A. Michalski, R.A. Scheltema, J.V. Olsen, M. Mann, Andromeda: a peptide search engine integrated into the MaxQuant environment, J. Proteome Res. 10 (4) (2011) 1794–1805.
[51] M. Ashburner, C.A. Ball, J.A. Blake, D. Botstein, H. Butler, J.M. Cherry, A.P. Davis, K. Dolinski, S.S. Dwight, J.T. Eppig, M.A. Harris, D.P. Hill, L. Issel-Tarver, A. Kasarskis, S. Lewis, J.C. Matese, J.E. Richardson, M. Ringwald, G.M. Rubin, G. Sherlock, Gene ontology: tool for the unification of biology, The Gene Ontology Consortium, Nat. Genet. 25 (1) (2000) 25–29.
[52] M. Kanehisa, S. Goto, KEGG: kyoto encyclopedia of genes and genomes, Nucleic Acids Res. 28 (1) (2000) 27–30.
[53] E.C. Yi, X.J. Li, K. Cooke, H. Lee, B. Raught, A. Page, V. Aneliunas, P. Hieter, D.R. Goodlett, R. Aebersold, Increased quantitative proteome coverage with (13)C/(12)C-based, acid-cleavable isotope-coded affinity tag reagent and modified data acquisition scheme, Proteomics 5 (2) (2005) 380–387.
[54] P.Y. Zeng, C.R. Vakoc, Z.C. Chen, G.A. Blobel, S.L. Berger, In vivo dual cross-linking for identification of indirect DNA-associated proteins by chromatin immunoprecipitation, BioTechniques 41 (6) (2006) 694. 696, 698.
[55] S.K. Kurdistani, M. Grunstein, In vivo protein-protein and protein-DNA crosslinking for genomewide binding microarray, Methods 31 (1) (2003) 90–95.
[56] J. Dejardin, R.E. Kingston, Purification of proteins associated with specific genomic Loci, Cell 136 (1) (2009) 175–186.